Received: 31 January 2018 | Accepted: 19 April 2018

DOI: 10.1111/jace.15723

Journal of the American Ceramic Society

ORIGINAL ARTICLE

Low-temperature sintering and thermal stability of Li_2GeO_3-based microwave dielectric ceramics with low permittivity

Changzhi Yin[1] | **Huaicheng Xiang**[1,2] | **Chunchun Li**[1,3] | **Harshit Porwal**[4] | **Liang Fang**[1]

[1]Guangxi Universities Key Laboratory of Non-ferrous Metal Oxide Electronic Functional Materials and Devices, College of Material Science and Engineering, Guilin University of Technology, Guilin, China

[2]Microelectronics Research Unit, Faculty of Information Technology and Electrical Engineering, University of Oulu, Oulu, Finland

[3]Materials Research Institute, Pennsylvania State University, University Park, State College, Pennsylvania

[4]School of Engineering and Material Science, Queen Mary University of London, London, UK

Correspondence
Chunchun Li and Liang Fang, Guangxi Universities Key Laboratory of Non-Ferrous Metal Oxide Electronic Functional Materials and Devices, College of Material Science and Engineering, Guilin University of Technology, Guilin, China.
Emails: lichunchun2003@126.com (CL) and fanglianggl001@aliyun.com (LF)

Funding information
Natural Science Foundation of China, Grant/Award Number: 51502047, 21561008, 21761008; Natural Science Foundation of Guangxi Zhuang Autonomous Region, Grant/Award Number: 2015GXNSFFA139003, 2016GXNSFBA380134, 2016GXNSFAA380018; Project of Scientific Research and Technical Exploitation Program of Guilin, Grant/Award Number: 2016010702-2, 20170225; Scholarship Fund of Guangxi Education Department.

Abstract

A low-permittivity dielectric ceramic Li_2GeO_3 was prepared by the solid-state reaction route. Single-phase Li_2GeO_3 crystallized in an orthorhombic structure. Dense ceramics with high relative density and homogeneous microstructure were obtained as sintered at 1000-1100°C. The optimum microwave dielectric properties were achieved in the sample sintered at 1080°C with a high relative density ~ 96%, a relative permittivity $\varepsilon_r \sim 6.36$, a quality factor $Q \times f \sim 29\,000$ GHz (at 14.5 GHz), and a temperature coefficient of resonance frequency $\tau_f \sim -72$ ppm/°C. The sintering temperature of Li_2GeO_3 was successfully lowered via the appropriate addition of B_2O_3. Only 2 wt.% B_2O_3 addition contributed to a 21.2% decrease in sintering temperature to 850°C without deteriorating the dielectric properties. The temperature dependence of the resonance frequency was successfully suppressed by the addition of TiO_2 to form Li_2TiO_3 with a positive τ_f value. These results demonstrate potential applications of Li_2GeO_3 in low-temperature cofiring ceramics technology.

KEYWORDS
ceramics, Li_2GeO_3, LTCC, microwave dielectric properties

Changzhi Yin and Huaicheng Xiang contributed equally to this work.

1 | INTRODUCTION

Microwave dielectric ceramics have been extensively used as key materials in dielectric resonators, filters, antennas, strip lines, and phase shifters for reasons of low cost, stability, efficiency, and ease of use.[1,2] Recently, to meet the increasing demands for miniaturization and integration, low-temperature cofired ceramics (LTCC) technology has become crucial due to its ability to integrate a versatile mix of passive microwave components to fabricate highly integrated multichip modules.[3-6] These ceramics must fulfill the requirement of lower sintering temperatures than the melting point of the inner metal electrode such as Ag (961°C), along with the appropriate relative permittivities (ε_r), high-quality factors ($Q \times f$), and temperature stability.[7,8] In addition, chemical compatibility of the ceramics with inner metal electrode should also be satisfied. LTCC technology has paved a way for the explosive progress of low-firing microwave dielectric ceramics.

Extensive literature reviewing reveals that the presence of low-melting-point constituents, such as Bi_2O_3, V_2O_5, GeO_2, Li_2CO_3, etc., is a common feature of the previously reported low-firing ceramics.[9-13] Herein, we are inspired to prepare Li_2GeO_3 consisting of Li_2O and GeO_2 with molar ratio 1:1 with an attempt to develop novel low-firing microwave dielectric ceramics. In the present work, Li_2GeO_3 ceramic was prepared using the solid-state reaction route and the sintering behavior, microstructure, and microwave dielectric properties were characterized.

2 | EXPERIMENTAL PART

The Li_2GeO_3 samples were synthesized by a solid-state reaction method. The initial reagents Li_2CO_3 (99.99%) and GeO_2 (99.999%) weighed with an accuracy of 0.003 g were mixed through ball milling using ZrO_2 balls with ethanol for 6 hours. The dried powder was pressed and fired in air at 900°C for 4 hours with 5°C/min, and remilled for 4 hours. The dried powder was added 10 mol.% PVA as a binder and pressed into 10 mm diameter and 5 mm height disks under a pressure of 200 MPa. The green compacts were firstly fired at 550°C in air for 2 hours to expel the organic binder and then sintered at 1000-1100°C for 4 hours.

Powder XRD data for the Li_2GeO_3 specimens were analyzed by X-ray diffractometer (X'Pert PRO, PANalytical, Almelo, Holland) using Cu Kα radiation. Cell parameters a, b, and c, and cell volume V were refined using the FULLFROF software. The surface microstructures of the pellets were observed by scanning electron microscopy (SEM, JSM6380-LV, Tokyo, Japan). The densities of the sintered ceramics were measured using the Archimedes method. The ε_r and $Q \times f$ values were measured in the TE_{011} mode according to the Hakki-Coleman method using an Agilent N5230A network analyzer (Palo Alto, CA). The temperature coefficient of resonate frequency τ_f value was measured from 25 to 85°C using a temperature chamber (Delta 9039, CA) and was calculated as follows:

$$\tau_f = \frac{f_{T_1} - f_{T_0}}{f_{T_0}(T_1 - T_0)} \quad (1)$$

where, f_{T_1} and f_{T_0} were the resonant frequencies at 85°C and room temperature, respectively.

3 | RESULTS AND DISCUSSION

Figure 1 shows the Rietveld refinement on the X-ray powder diffraction pattern of the calcined Li_2GeO_3 at 900°C/4 h. The Rietveld refinement was performed with the Fullprof program based on the XRD data and a starting model from Ref. [14] was used for the structural refinement. The excellent agreement between the calculated and observed XRD profiles and the low residual factors (Rp = 2.46%, Rwp = 4.22%) confirm the phase purity of Li_2GeO_3 and indicate the formation of single-phase Li_2GeO_3 with a space group *Cmc21* (36). The schematic crystal structure of Li_2GeO_3 is shown in the inset of Figure 1, where the ionic arrangement can be clearly shown. The structure is composed of the hexagonal close-packed oxygen and cations ordered on 1 set of distorted tetrahedral sites. In the structure, Li^+ and Ge^{4+} are placed at Wyckoff positions 8b and 4a, respectively; and the oxygen locates at 4a and 8b positions. On the basis of Rietveld refinement, the lattice parameters are refined as a = 9.6316(7) Å, b = 5.47917(7) Å, c = 4.8417(8) Å, and V = 255.5180(1) $Å^3$. The theoretical density was obtained from the crystal structure and atomic weight and yielded a value of 3.496 g/cm^3.

Scanning electron microscopy micrographs recorded from the polished and thermal etched surfaces of the Li_2GeO_3 ceramics sintered at 1020-1100°C are shown in Figure 2. It is evident that no additional phases are visible in the SEM images, which is consistent with the XRD analysis. Visible pores could be observed in the low-temperature sintered samples, as shown in Figure 2A. The amount of porosity declined obviously with increasing sintering temperature accompanied by a clear increase in grain size. A densified microstructure with well-packed grains and legible grain boundaries was developed in the sample sintered at 1080°C and the average grain size was about 5-10 μm. However, abnormal grain growth occurred when sintered at 1100°C characterized by extremely large grains ~20 μm and microcracks, which might deteriorate the dielectric properties in Li_2GeO_3 ceramics.

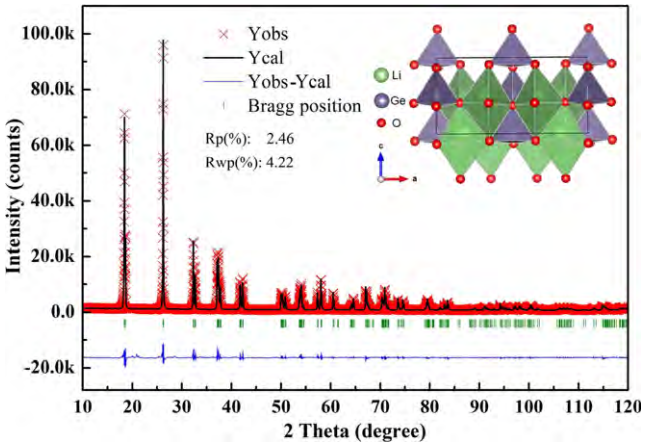

FIGURE 1 The Rietveld refinement on the X-ray powder diffraction pattern of the calcined Li_2GeO_3 at 900°C/4 h (the structure diagram of Li_2GeO_3 is given in the inset)

Figure 3 shows the variation in relative density and microwave dielectric properties (ε_r, $Q \times f$, and τ_f) of Li_2GeO_3 ceramics as a function of sintering temperature ranging from 1000 to 1100°C in 20°C increments. The relative density showed an increased tendency with the increasing sintering temperature and reached a saturated value of 96% at 1080°C. The increase in density is due to the decrease of porosity and the homogenous grain size. However, it should be noted that Li_2GeO_3 has a narrow densification sintering temperature intervals. A slight increase in sintering temperature to 1100°C decreased the relative density. This can be explained by the abnormal grain growth observed in the 1100°C sintered sample. Combined with the SEM analysis, sintering at 1080°C was determined to be the optimum sintering condition.

As shown in Figure 3B, the variation in relative permittivity (ε_r) is consistent with the density. The higher density corresponds to higher dielectric constant. A maximum value of $\varepsilon_r = 6.36$ was obtained at 1080°C. It is well known that the microwave relative permittivity can be affected not only by the intrinsic factors (crystal symmetry, dielectric polarizability, etc.) but also by the extrinsic factors, such as secondary phase, density, porosity, grain size, etc.[15-17] In the present work, the dependence of ε_r on density demonstrates that porosity plays a dominant role in affecting the relative permittivity. To eliminate the influence of porosity, the relative permittivity was porosity corrected by using the Bosman and Having's equation: $\varepsilon_{corr} = \varepsilon_r (1 + 1.5p)$ with p the fractional porosity. For the sample sintered at 1080°C, the ε_{corr} value was 6.74. According to the Clausius-Mossotti relationship and Shannon's additive law, the theoretical dielectric constant can be estimated.[18,19] The theoretical permittivity of Li_2GeO_3 was calculated to be 6.81. The relative error

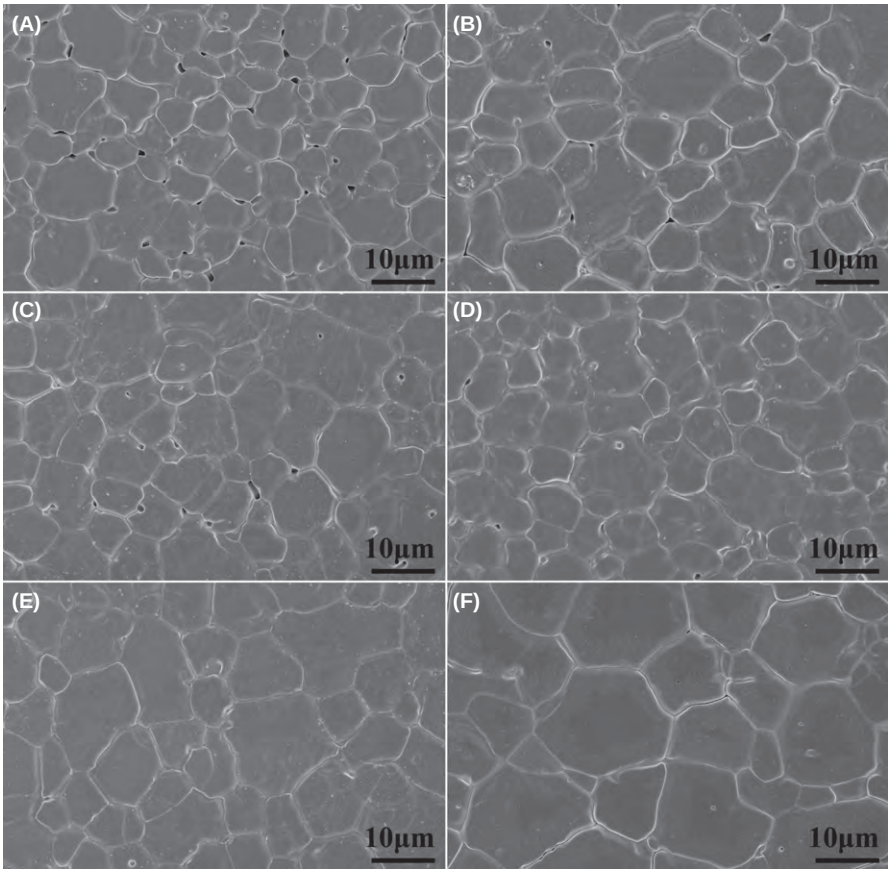

FIGURE 2 SEM micrographs of the polished and thermal etched surfaces of the Li_2GeO_3 ceramics sintered at (A) 1000°C, (B) 1020°C, (C) 1040°C, (D) 1060°C, (E) 1080°C, and (F) 1100°C

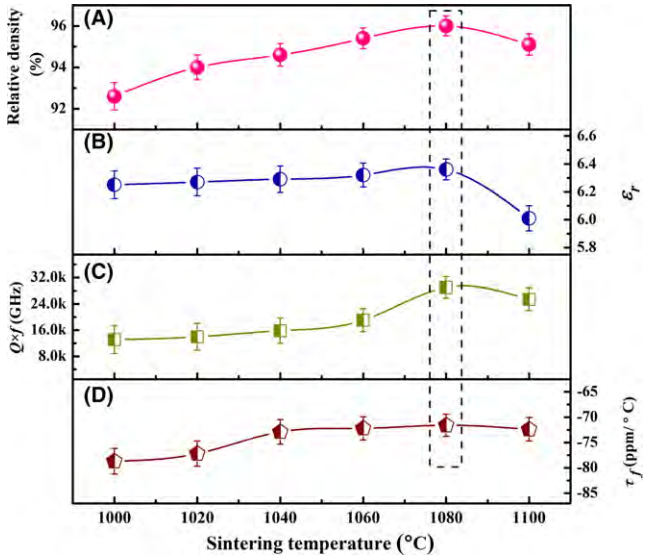

FIGURE 3 The variation in relative density (A) and microwave dielectric properties of Li_2GeO_3 ceramics as a function of sintering temperature from 1000 to 1100°C in 20°C increments: (B)ε_r, (C) $Q \times f$, and (D) τ_f

between the porosity corrected and theoretical permittivity is 1.1%. The small deviation indicates that ionic polarization plays a prominent role in the dielectric polarizability at microwave frequency region.

Figure 3C shows the variation in quality factor ($Q \times f$) of Li_2GeO_3 ceramics sintered at different temperatures. Similar to the relative permittivity, the quality factor exhibited obvious dependence on sintering temperature. With increasing sintering temperature, the quality factor of Li_2GeO_3 increased continuously to a maximum value of 29 000 GHz at 1080°C and thereafter decreased. The enhanced $Q \times f$ value is attributed to the decreased porosity with increasing sintering temperature. Further increase in sintering temperature to 1100°C induced abnormal grain growth, leading to inhomogeneous microstructure and reappearing porosity, which in turn deteriorate the quality factor. As shown in Figure 3D, no obvious dependence on sintering temperature was observed for the τ_f value and it remained between −71 and −78 ppm/°C. This mainly because no structural changed happened over the sintering temperature range of 1000-1100°C.

Nevertheless, the sintering temperature is still too high for application in LTCC technology to cofire the low-cost silver electrodes. Thus, to lower the sintering temperature, a small amount of B_2O_3 was added to Li_2GeO_3. As shown in Figure 4, XRD patterns of the 2 wt.% B_2O_3-doped ceramic was consistent with the parent Li_2GeO_3 and all the observed peaks could be indexed, whereas the 5 wt.% B_2O_3-doped sample exhibited a secondary phase, $LiBGeO_4$ (JCPDS No. 01-074-2079), with a characteristic peak at ~23°. This result indicates that Li_2GeO_3 reacted with B_2O_3 at 850°C. And the chemical reaction is as follows:

$$2Li_2GeO_3 + B_2O_3 \xrightarrow{820°C} LiBGeO_4 + Li_2O \qquad (2)$$

The back scattered SEM (BSEM) image on the Li_2GeO_3 + 2 wt.% B_2O_3 demonstrates that B_2O_3 doping promoted the grain growth, as shown in the inset of Figure 4. The sintering temperature and microwave dielectric properties of x wt.% B_2O_3-doped Li_2GeO_3 are summarized in Table 1. As expected, B_2O_3 addition successfully reduced the sintering temperature of Li_2GeO_3. Only 2 wt.% B_2O_3 addition contributed to a 21.2% decrease in sintering temperature to 850°C. The 2 wt.% B_2O_3 added Li_2GeO_3 ceramic exhibited encouraging microwave dielectric properties with $\varepsilon_r = 5.57$ along with $Q \times f = 13\ 800$ GHz and $\tau_f = -82$ ppm/°C when sintered at 850°C. Compared with the pure Li_2GeO_3 ceramic, however, B_2O_3 addition had an adverse effect on the microwave dielectric properties, mainly owing to the larger grain size and the amorphous phase appeared during liquid-phase sintering. In addition, it is assumed that the extremely low quality factor and the temperature coefficient of the resonance frequency of the 5 wt.% B_2O_3 added Li_2GeO_3 ceramic was partially related to the secondary phase $LiBGeO_4$ that might have a low ε_r and τ_f values. Further work to confirm the microwave dielectric properties of $LiBGeO_4$ is ongoing.

In the viewpoint of technological applications, the temperature dependence of the Li_2GeO_3 ceramics is extremely low with a largely negative τ_f value and must be suppressed. Several approaches, for example, ionic substitution, composite forming, or microstructural engineering have been proposed to tune the τ_f value.[20-22] TiO_2 was chosen to compensate the negative τ_f of Li_2GeO_3 because

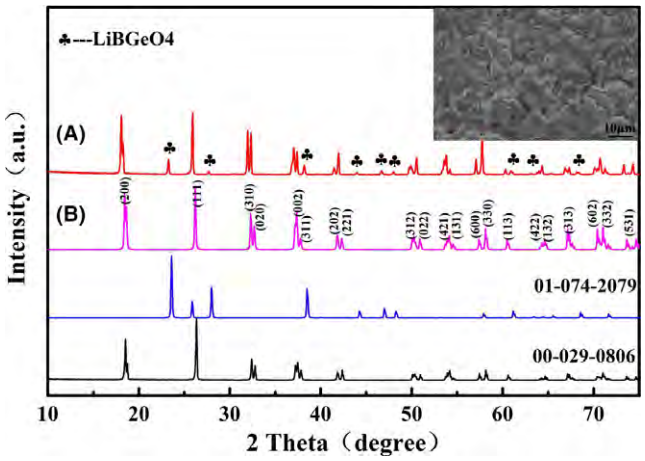

FIGURE 4 XRD patterns of the Li_2GeO_3 ceramics with (A) 5 wt.% B_2O_3 and (B) 2 wt.% B_2O_3 (inset is the SEM image of the Li_2GeO_3 ceramics with 2 wt.% B_2O_3 doping and sintered at 850°C)

TABLE 1 Sintering temperature, bulk density, and microwave dielectric properties of x wt.% B_2O_3-doped Li_2GeO_3 ceramics

x value	S. T. (°C)	ε_r	$Q \times f$ (GHz)	τ_f (ppm/°C)
0	1080	6.36	29 000	−72
2	850	5.57	13 800	−82
5	820	5.23	7750	−108.8

of its large positive τ_f value (~+465 ppm/°C) and the chemical similarity of Ti^{4+} to Ge^{4+}. The choice of TiO_2 was also guided by its successful applications in compensating the temperature stability of other materials.[23,24] Four different compositions with $y = 0.2, 0.4, 0.6, 0.8$ in the formula $Li_2Ge_{1-y}Ti_yO_3$ were prepared and characterized. XRD analysis, as shown in Figure 5, demonstrates that all the ceramics were comprised of 2 phases: Li_2GeO_3 and a rock salt Li_2TiO_3. With increasing y value, the fraction of rock salt phase increased characterized by the increasing strongest diffraction peak at $2\theta \sim 44^{\circ}$. As clearly detected, some XRD peaks overlapped, and thus Raman spectra analysis was employed to further confirm the phase constituent due to its sensibility to structural change compared to the XRD analysis. Figure 6 shows the Raman spectra for the $Li_2Ge_{1-y}Ti_yO_3$ ($y = 0.2, 0.4, 0.6, 0.8$) ceramics and the spectroscopy for the nominal Li_2GeO_3 is also given for comparison. In the range 100-1100 cm^{-1}, all the observed Raman modes can be assigned to the Li_2GeO_3 phase (marked with the dot lines) and the Li_2TiO_3 phase (marked with the rectangular). The indexing of the modes for Li_2TiO_3 is based on the previous reports.[25,26] These results indicate that only 2 phases, Li_2GeO_3 and Li_2TiO_3, were found in the $Li_2Ge_{1-y}Ti_yO_3$ system.

To obtain the precise percentage of Li_2TiO_3, a quantitative Rietveld analysis was carried out based on the XRD data of the $Li_2Ge_{1-y}Ti_yO_3$. Representative plots of the observed and calculated diffraction patterns performed on the $y = 0.4$ sample are given in Figure 7 as well as the Brag positions. The two-phase Rietveld refinement yielded 37.8 mol.% and 62.2 mol.% for Li_2TiO_3 and Li_2GeO_3, respectively. The fractions of the rock salt Li_2TiO_3 phase based on the Rietveld refinement are 18.1%, 37.8%, 58.3%, and 77.9% for $y = 0.2$, 0.4, 0.6, and 0.8, respectively. It should be noted that the percentage of Li_2TiO_3 is slightly lower than the nominal percentage (the y value), which means there is a small amount of Ti dissolved into Li_2GeO_3 to form the solid solution and the solubility was around 1.7%-2.1%. Li_2TiO_3 was reported to have a positive τ_f value of ~ 20 ppm/°C along with an extremely low dielectric loss.[27] Thus, it is expected that the thermal stability of Li_2GeO_3 could be tuned by forming composite ceramics with Li_2TiO_3.

Figure 7 lists the ε_r, $Q \times f$, and τ_f values of the $Li_2Ge_{1-y}Ti_yO_3$ ceramics as a function of y value. As expected, the τ_f values of $Li_2Ge_{1-y}Ti_yO_3$ ceramics increased with the y values and shifted from negative to positive. A near-zero τ_f value of +2.9 ppm/°C was obtained in the $y = 0.8$ composite when sintered at 1100°C. This is because the Li_2TiO_3 ceramic sintered at 1230°C obtained a τ_f value of about +38.5 ppm/°C,[28] which also indicates that Li_2TiO_3 could well compensate for the τ_f value of Li_2GeO_3. As shown, the ε_r value also increased with increasing Li_2TiO_3 content, which is attributed to the higher ε_r value of Li_2TiO_3 (~22.1). For a binary phase composite, the theoretical ε_r and τ_f values can be evaluated according to the empirical Lichtenecker logarithmic rule[29]:

$$\ln\varepsilon = x_1 \ln\varepsilon_1 + x_2 \ln\varepsilon_2 \tag{3}$$

$$\tau_f = x_1\tau_{f1} + x_2\tau_{f2} \tag{4}$$

where x_1 and x_2 are the volume fractions, ε_1 and ε_2 are the permittivities, τ_{f1} and τ_{f2} are the τ_f values of the pure Li_2GeO_3 and Li_2TiO_3 phase, respectively. The calculated ε_r

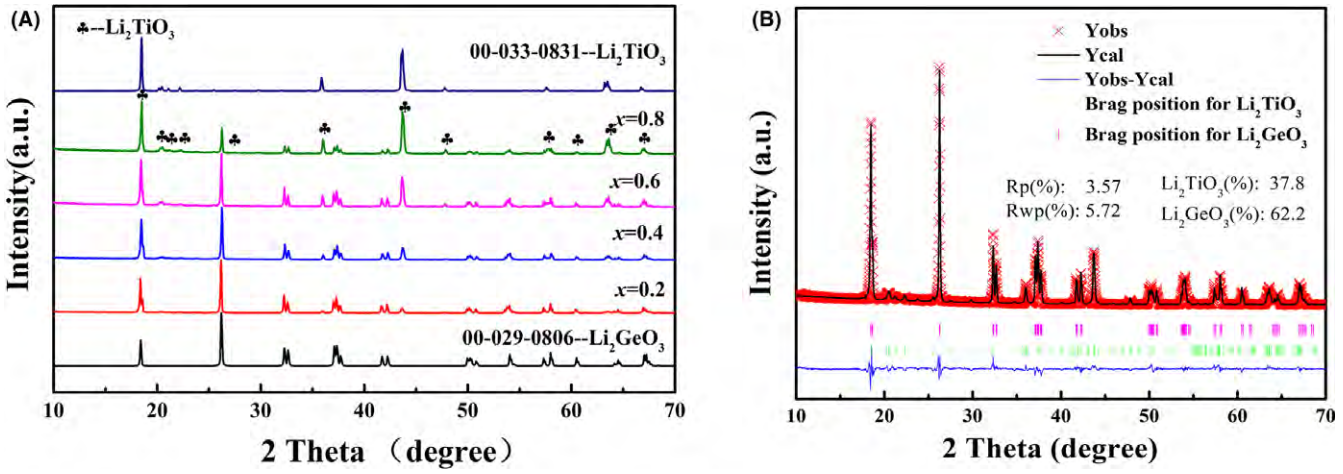

FIGURE 5 (A) XRD patterns of the $Li_2Ge_{1-y}Ti_yO_3$ ($y = 0.2, 0.4, 0.6, 0.8$) sintered at 1100°C; (B) The Rietveld refinement on the $Li_2Ge_{0.6}Ti_{0.4}O_3$ sample

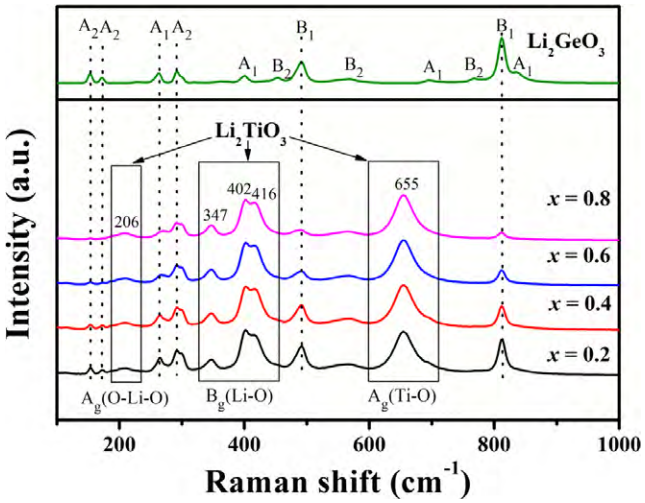

FIGURE 6 Raman spectra for the $Li_2Ge_{1-y}Ti_yO_3$ (y = 0.2, 0.4, 0.6, 0.8) ceramics as well as the nominal Li_2GeO_3

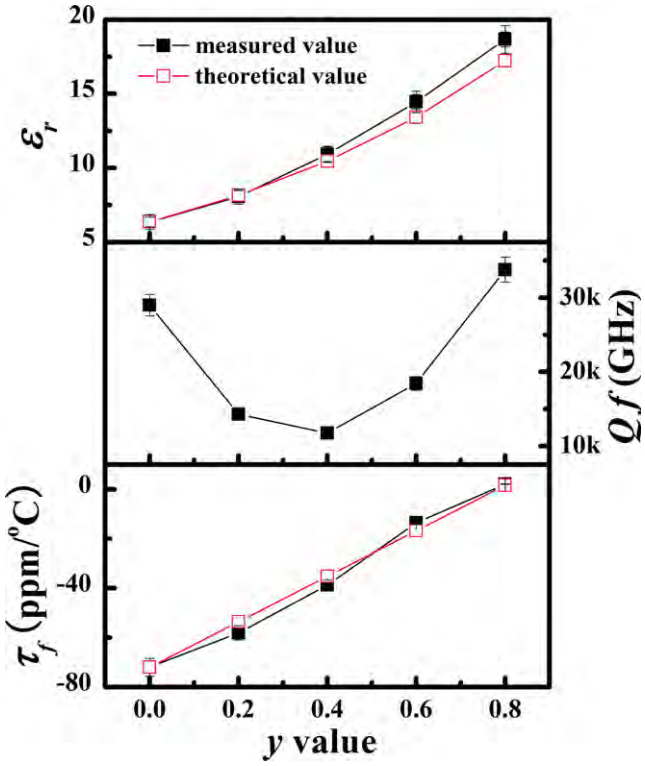

FIGURE 7 The ε_r, theoretical ε_r, $Q \times f$, τ_f, and theoretical τ_f values of $Li_2Ge_{1-y}Ti_yO_3$ ceramics as a function of the y values

and τ_f values are also given in Figure 7. By comparison, the measured values coincide with the calculated values. On the other hand, the τ_f value is reported to be closely related to the chemical nature of ions, the distance between cations and anions.[30] The slight deviation might be related to the solid solution between Ti and Ge which should lead to the change in the bond distance and structural distortion. The quality factor also exhibited a strong dependence on the composition, which decreased with increasing y value to a minimum value of 11 750 GHz at $y = 0.4$ but increased thereafter to 33 790 GHz at $y = 0.8$. It should be noted that even though the quality factor of the $y = 0.8$ composite is much higher than the end member Li_2GeO_3 but inferior to the other end member Li_2TiO_3 with a $Q \times f$ = 63 500 GHz. It is well accepted that the quality factor of the dielectric ceramics strongly depends on the densification, porosity, grain size, phase evolution, etc.[31,32] In the present case, the internal mismatch or strain because of the coexistence of 2 phases with different structures dominates the variation in the quality factor. In addition, the grain boundaries due to the heterostructure would increase the dielectric losses as 2D defects. In summary, a composite with $y = 0.8$ exhibited a good combination of microwave dielectric properties with $\varepsilon_r \sim 18.67$, $Q \times f \sim 33\ 790$ GHz, and $\tau_f \sim +2.1$ ppm/°C.

4 | CONCLUSIONS

Li_2GeO_3 ceramics were prepared by the solid-state reaction method and the crystal structure, microstructure, and microwave dielectric properties were characterized. Single-phase ceramics with orthorhombic structure and homogeneous microstructure were obtained when sintered at 1080°C. Good microwave dielectric properties with $\varepsilon_r \sim 6.36$, a $Q \times f \sim 29\ 000$ GHz (at 14.5 GHz), and $\tau_f \sim -72$ ppm/°C were achieved in the Li_2GeO_3 ceramic sintered at 1080°C. An appropriate amount of B_2O_3 addition successfully reduced the sintering temperature of Li_2GeO_3 to 850°C. The Li_2GeO_3 + 2wt% B_2O_3 exhibited good dielectric performances with $\varepsilon_r \sim 5.57$, $Q \times f \sim 13\ 800$ GHz, and $\tau_f \sim -82$ ppm/°C when sintered at 850°C, showing potential applications in low-temperature cofiring ceramics technology. In addition, the temperature dependence of the resonance frequency was successfully suppressed by the addition of TiO_2 to form Li_2TiO_3 with a positive τ_f value. A composite with $y = 0.8$ in $Li_2Ge_{1-y}Ti_yO_3$ exhibited good combination of microwave dielectric properties with $\varepsilon_r \sim 18.67$, $Q \times f \sim 33\ 790$ GHz, and $\tau_f \sim +2.1$ ppm/°C.

ACKNOWLEDGMENTS

This work was supported by Natural Science Foundation of China (Nos. 51502047, 21561008, and 21761008), the Natural Science Foundation of Guangxi Zhuang Autonomous Region (Nos. 2015GXNSFFA139003, 2016GXNSFBA380134, and 2016GXNSFAA380018), Project of Scientific Research and Technical Exploitation Program of Guilin (20160-10702-2 and 20170225). Chunchun Li gratefully acknowledges the Guangxi Scholarship Fund of Guangxi Education Department.

ORCID

Chunchun Li http://orcid.org/0000-0002-3657-5856

REFERENCES

1. Sebastian MT. Dielectric Materials for Wireless Communication. Oxford: Elsevier; 2008.
2. Varghese J, Siponkoski T, Teirikangas M, Sebastian MT, Uusimaki A, Jantunen H. Structural, dielectric, and thermal properties of Pb free molybdate based ultralow temperature glass. *ACS Sustainable Chem Eng*. 2016;4:3897-3904.
3. Jantunen H, Rautioaho R, Uusimaki A, Leppavuori S. Compositions of $MgTiO_3$-$CaTiO_3$ ceramic with two borosilicate glasses for LTCC applications. *J Eur Ceram Soc*. 2000;20:2331-2336.
4. Lei W, Lu WZ, Wang XC. Temperature compensating $ZnAl_2O_4$-Co_2TiO_4 spinel-based low-permittivity microwave dielectric ceramics. *Ceram Int*. 2012;38:99-103.
5. Joseph N, Varghese J, Siponkoski T, Teirikangas M, Sebastian MT, Jantunen H. Glass-free $CuMoO_4$ ceramic with excellent dielectric and thermal properties for ultralow temperature cofired ceramic applications. *ACS Sustain Chem Eng*. 2016;4:5632-5639.
6. Zhou D, Randall CA, Wang H, Pang LX, Yao X. Microwave dielectric ceramics in Li_2O-Bi_2O_3-MoO_3 system with ultra-low sintering temperatures. *J Am Ceram Soc*. 2010;93:1096-1100.
7. Xiang HC, Fang L, Jiang XW, Tang Y, Li CC. A novel temperature stable microwave dielectric ceramic with garnet structure: $Sr_2NaMg_2V_3O_{12}$. *J Am Ceram Soc*. 2016;99:399-401.
8. Xiang HC, Li CC, Tang Y, Fang L. Two novel ultralow temperature firing microwave dielectric ceramics $LiMVO_6$ (M = Mo, W) and their chemical compatibility with metal electrodes. *J Eur Ceram Soc*. 2017;37:3959-3963.
9. Zhou D, Guo D, Li WB, et al. Novel temperature stable high-ε_r microwave dielectrics in the Bi_2O_3-TiO_2-V_2O_5 system. *J Mater Chem C*. 2016;4:5357-5362.
10. Li CC, Xiang HC, Tang Y, et al. Low-firing and temperature stable microwave dielectric ceramics: $Ba_2LnV_3O_{11}$ (Ln = Nd, Sm). *J Am Ceram Soc*. 2018;101:773-781.
11. Valan M, Popovic J, Mihelj MV, Burazer S, Altomare A, Moliterni A. Oxide crystal structure with square-pyramidally coordinated vanadium for integrated electronics manufactured at ultralow processing temperatures. *ACS Sustainable Chem Eng*. 2017;5:5662-5668.
12. Li CC, Xiang HC, Xu MY, Tang Y, Fang L. Li_2AGeO_4 (A = Zn, Mg): two novel low-permittivity microwave dielectric ceramics with olivine structure. *J Eur Ceram Soc*. 2018;38:1524-1528.
13. Zhou D, Randall CA, Pang LX, et al. Microwave dielectric properties of Li_2WO_4 ceramic with ultra-low sintering temperature. *J Am Ceram Soc*. 2011;94:348-350.
14. Ikeda T, Imazu I. Piezoelectric study of Li_2GeO_3 crystal. *Jpn J Appl Phys*. 1976;15:1451-1454.
15. Huang CL, Huang SH. Low-loss microwave dielectric ceramics in the $(Co_{1-x}Zn_x)TiO_3$ (x = 0-01) system. *J Alloys Compd*. 2012;515:8-11.
16. Cao QS, Lu WZ, Wang XC, Zhu JH, Ulla B, Lei W. Novel zinc manganese oxide-based microwave dielectric ceramics for LTCC applications. *Ceram Int*. 2015;41:9152-9156.
17. Zou ZY, Chen ZH, Lan XK, et al. Weak ferroelectricity and low-permittivity microwave dielectric properties of $Ba_2Zn_{(1+x)}$-$Si_2O_{(7+x)}$ ceramics. *J Eur Ceram Soc*. 2017;37:3065-3071.
18. Shannon RD. Dielectric polarizabilities of ions in oxides and fluorides. *J Appl Phys*. 1993;73:348-366.
19. Yoon SH, Kim DW, Cho SY, Hong KS. Investigation of the relations between structure and microwave dielectric properties of divalent metal tungstate compounds. *J Eur Ceram Soc*. 2006;26:2051-2054.
20. Zhou D, Pang LX, Wang H, Guo J, Yao X, Randall CA. Phase transition, Raman spectra, infrared spectra, band gap and microwave dielectric properties of low temperature firing $(Na_{05x}Bi_{1-05x})(Mo_xV_{1-x})O_4$ solid solution ceramics with scheelite structures. *J Mater Chem*. 2011;21:18412-18420.
21. Wang XC, Lei W. Ang R, Lu WZ. $ZnAl_2O_4$-TiO_2-$SrAl_2Si_2O_8$ low-permittivity microwave dielectric ceramics. *Ceram Int*. 2013;39:1707-1710.
22. Xiang HC, Fang L, Xu MY, Tang Y, Li CC. Microwave dielectric properties of $Na_{2x}Ba_{1-x}Li_2Ti_6O_{14}$ ceramics and their chemical compatibility with silver. *Mater Chem Phys*. 2017;195:275-282.
23. Ullah A, Liu HX, Hao H, Iqbal J, Yao ZH, Cao MH. Influence of TiO_2 additive on sintering temperature and microwave dielectric properties of $Mg_{090}Ni_{01}SiO_3$ ceramics. *J Eur Ceram Soc*. 2017;37:3045-3049.
24. Zheng HR, Yu SH, Li LX, Lyu XS, Sun Z, Chen SL. Crystal structure, mixture behavior, and microwave dielectric properties of novel temperature stable $(1\text{-}x)MgMoO_4-xTiO_2$ composite ceramics. *J Eur Ceram Soc*. 2017;37:4661-4665.
25. Ding YM, Bian JJ. Structural evolution, sintering behavior and microwave dielectric properties of $(1-x)Li_2TiO_3$ + xLiF ceramics. *Mater Res Bull*. 2013;48:2776-2781.
26. Li W, Fang L, Tang Y, Sun YH, Li CC. Microwave dielectric properties in the $Li_{4+x}Ti_5O_{12}$ $(0 \le x \le 12)$ ceramics. *J Alloys Compd*. 2017;701:295-300.
27. Yuan LL, Bian JJ. Microwave dielectric properties of the lithium containing compounds with rock salt structure. *Ferroelectrics*. 2009;387:123-129.
28. Pang LX, Zhou D. Microwave dielectric properties of low-firing Li_2MO_3 (M = Ti, Zr, Sn) ceramics with B_2O_3-CuO addition. *J Am Ceram Soc*. 2010;93:3614-3617.
29. Wu Y, Zhou D, Guo J, Pang LX, Wang H, Yao X. Temperature stable microwave dielectric ceramic $03Li_2TiO_3$-$07Li(Zn_{05}Ti_{15})O_4$ with ultra-low dielectric loss. *Mater Lett*. 2011;65:2680-2682.
30. Kim WS, Yoon KH. Microwave dielectric properties and far-infrared reflectivity characteristics of the $CaTiO_3$–$Li_{1/2-3x}Sm_{1/2+x}TiO_3$ ceramics. *J Am Ceram Soc*. 2000;83:2327-2329.
31. Bi JX, Niu YJ, Wu HT. $Li_4Mg_3Ti_2O_9$: a novel low-loss microwave dielectric ceramic for LTCC applications. *Ceram Int*. 2017;43:7522-7530.
32. Lei W, Ang R, Wang XC, Lu WZ. Phase evolution and near-zero shrinkage in $BaAl_2Si_2O_8$ low-permittivity microwave dielectric ceramics. *Mater Res Bull*. 2014;50:235-239.

How to cite this article: Yin C, Xiang H, Li C, Porwal H, Fang L. Low-temperature sintering and thermal stability of Li_2GeO_3-based microwave dielectric ceramics with low permittivity. *J Am Ceram Soc*. 2018;00:1–7. https://doi.org/10.1111/jace.15723